

# Capacitive coupling of two transmission line resonators mediated by the phonon number of a nanoelectromechanical oscillator

O. P. de Sá Neto,<sup>1,2,\*</sup> M. C. de Oliveira,<sup>2,†</sup> F. Nicacio,<sup>2</sup> and G. J. Milburn<sup>3</sup>

<sup>1</sup>*Coordenação de Ciência da Computação, Universidade Estadual do Piauí, CEP 64202220 Parnaíba, Piauí, Brazil*

<sup>2</sup>*Instituto de Física Gleb Wataghin, Universidade Estadual de Campinas, 13083-970 Campinas, São Paulo, Brazil*

<sup>3</sup>*Centre of Excellence in Engineered Quantum Systems, University of Queensland, Queensland 4072, Brisbane, Australia*

(Received 6 May 2014; published 25 August 2014)

Detection of quantum features in mechanical systems at the nanoscale constitutes a challenging task, given the weak interaction with other elements and the available technology. Here we describe the interaction between two monomodal transmission-line resonators (TLRs) mediated by vibrations of a nanoelectromechanical oscillator. This scheme is then employed for quantum nondemolition detection of the number of phonons in the nanoelectromechanical oscillator through a direct current measurement in the output of one of the TLRs. For that to be possible an undepleted field inside one of the TLRs works as an amplifier for the interaction between the mechanical resonator and the remaining TLR. We also show how the nonclassical nature of this system can be used for generation of tripartite entanglement and conditioned mechanical coherent superposition states, which may be further explored for detection processes.

DOI: [10.1103/PhysRevA.90.023843](https://doi.org/10.1103/PhysRevA.90.023843)

PACS number(s): 42.50.Wk, 42.50.Lc, 85.85.+j

## I. INTRODUCTION

The nature of the movement of tiny electromechanical oscillators has proved very intriguing, receiving attention since the early years of quantum theory [1]. Recently, several groups have been able to engineer nanoelectromechanical systems (NEMSs) with oscillation frequencies up to the gigahertz scale, despite the challenge to sensitively detect movement at that small scale [2–6]. Indeed it was demonstrated recently that one can cool down to almost the ground state of the mechanical oscillator [7–9] and implement experiments near the zero-point motion [10], therefore inside the quantum regime. Single electron transistor devices are the natural choice for movement detection, but recently electrical transducers of motion using circuit quantum electrodynamic devices have been considered [11,12]. Indeed, it is interesting to explore the possibilities that a transduction and coupling to other circuit elements may offer for detection purposes.

In this article we show that a direct capacitive coupling between a mechanical oscillator and two transmission-line resonators (TLRs) [13] enables a quadratic coupling between the TLRs and the mechanical displacement. This procedure leads to an efficient method for measurement of the mean phonon number of the mechanical oscillator by current measurements on the device. The coupling between the mechanical oscillator and the radiation field inside the resonators is amplified in an undepleted regime, allowing a direct quantum nondemolition (QND) measurement of the mechanical resonator mean number of phonons in a simple setup. As a secondary result, given the nature of the interaction between the elements, an entangled state can be generated between the TLR modes and the mechanical resonator states, which might be useful for further application in quantum-information processing, or for detection purposes.

## II. MODEL

Quantum features for a mechanical oscillator manifest only when its oscillation frequency  $\nu$  reaches the  $\nu > k_B T/\hbar$  limit. For typical temperatures of a few millikelvins,  $\nu$  must be of the order of gigahertz. Since  $\nu \propto l^{-1}$ , where  $l$  is a typical dimension of the oscillator, this requires  $l$  to be of the order of a few nanometers. To test the quantum nature of those oscillations constitutes a real challenge. A natural way for probing it is through the direct electrical coupling of the mechanical oscillator to radiation at the microwave scale, as has been recently demonstrated [7,10,14]. In those cases standard electrical measurements can be used to monitor the mechanical oscillations. In the same spirit, we consider two TLRs capacitively coupled to a mechanical oscillator as depicted in Fig. 1. Since the capacitance changes with the distance, the mechanical oscillations of the NEMS change the distributed capacitances of the circuit:  $C_L(t) = \frac{\epsilon_0 A}{[d-x(t)]}$  between TLR 1 and the NEMS and  $C_R(t) = \frac{\epsilon_0 A}{[d+x(t)]}$  between TLR 2 and the NEMS, where  $\epsilon_0$  is the vacuum dielectric constant,  $A$  is the lateral area of the NEMS, and  $d$  is the equilibrium distance of both TLRs from the NEMS, here assumed to be equal. Also  $x(t)$  is the time-dependent displacement of the NEMS from its center of mass. At the NEMS's equilibrium position, we define the equilibrium capacitance as  $C_{eq} = \epsilon_0 A/d$  and we avoid a short circuit by stating that  $\max |x(t)| < d$ .

By considering the distributed voltage and current in the corresponding circuit, after some algebraic manipulations we derive the system Hamiltonian [see the appendixes for a complete derivation of Hamiltonians (1) and (5)],

$$\mathcal{H} = \frac{1}{2} \sum_{i=1}^2 \left( \frac{1}{L_i} P_i^2 + \frac{1}{C_i} Q_i^2 \right) + \frac{[d^2 - x^2(t)]}{2d\epsilon_0 A} Q_1 Q_2 - \sum_{i=1}^2 \left[ \frac{[(-1)^i d + x(t)]}{2d} V_{C_T}(t) \right] Q_i, \quad (1)$$

\*olimpioqedc@gmail.com

†marcos@ifi.unicamp.br

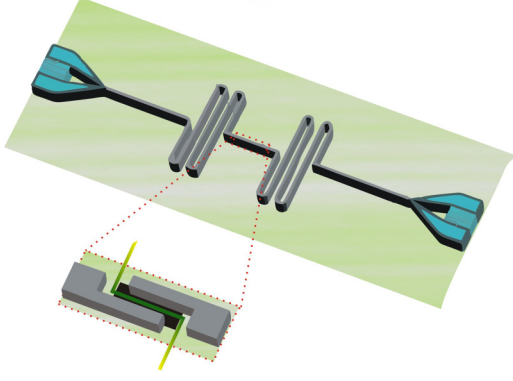


FIG. 1. (Color online) Capacitive coupling of two TLRs mediated by an oscillatory NEMS. A double clamped mechanical resonator (green) is electrically coupled to two transmission line resonators (grey).

where  $Q_i$ ,  $P_i$ , and  $L_i$  are, respectively, the charge, the magnetic flux, and the impedance at the TLR,  $i = 1, 2$ . We have also defined  $V_{C_T} \equiv V_{C_L} - V_{C_R} = Q_L(t)C_L(t)^{-1} - Q_R(t)C_R(t)^{-1}$ , and  $\tilde{C}_i^{-1} \equiv C_i^{-1} + \frac{[d^2 - x^2(t)]}{2d\epsilon_0 A}$ , where  $C_i$  is the capacitance in each TLR,  $i = 1, 2$ . In that Hamiltonian we have assumed that only one mode on each TLR is significant in the coupling with the NEMS fundamental mode, as depicted in Fig. 2.

Before full quantization of Eq. (1), we assume a regime of rapid oscillation of the NEMS, by writing

$$x(t) = \sqrt{\frac{\hbar}{2mv}}(be^{-i\omega t} + b^\dagger e^{i\omega t}). \quad (2)$$

For rapid oscillations ( $\omega t \gg 1$ ),  $\langle x(t) \rangle \approx 0$ ; furthermore,  $\langle x^2(t) \rangle \approx \frac{\hbar}{mv} \langle (b^\dagger b) + \frac{1}{2} \rangle \equiv x_{\text{rms}}^2$ . Thus a relation between the frequencies  $\omega_i^2 \equiv (L_i C_i)^{-1}$  and  $\tilde{\omega}_i^2 \equiv (L_i \tilde{C}_i)^{-1}$  is obtained as

$$\tilde{\omega}_i^2 = \omega_i^2 + \frac{\omega_{i,\text{eq}}^2}{2} \left( 1 - \frac{x_{\text{rms}}^2}{d^2} \right), \quad (3)$$

where  $\omega_{i,\text{eq}}^2 \equiv (C_{\text{eq}} L_i)^{-1}$ . For the sort of device we are looking for, it is reasonable to assume  $x_{\text{rms}}^2/d^2 = 10^{-6}$  [15,16] and we disregard it from Eq. (3) in a first approximation. Typical experimental values settle  $\omega_i = 6$  GHz [15], and if the second term in Eq. (3) is of the same order it should also be taken into account. We keep the maximal value the second term can take, adopting  $\tilde{\omega}_i^2 = \omega_i^2 + \omega_{i,\text{eq}}^2/2$ , meaning that

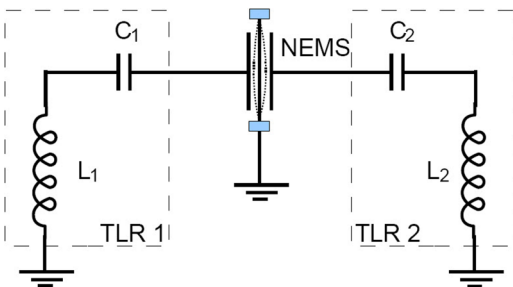


FIG. 2. (Color online) Schematic circuit corresponding to Hamiltonian (1); a single-mode approximation was considered for both the TLRs and the NEMS.

$\tilde{C}_i^{-1} = C_i^{-1} + (2C_{\text{eq}})^{-1}$ . Assuming

$$Q_j = \sqrt{\frac{\hbar}{2L_j \tilde{\omega}_j}}(a_j^\dagger + a_j) \quad \text{and} \quad P_j = i\sqrt{\frac{\hbar L_j \tilde{\omega}_j}{2}}(a_j^\dagger - a_j), \quad (4)$$

which follow the standard commutation relation, we obtain

$$H = H_0 + H_{\text{int}} + H_d, \quad (5)$$

where

$$H_0 = \hbar \tilde{\omega}_1 (a_1^\dagger a_1 + \frac{1}{2}) + \hbar \tilde{\omega}_2 (a_2^\dagger a_2 + \frac{1}{2}), \quad (6)$$

$H_{\text{int}}$  is the coupling between the two TLRs mediated by the NEMS phonon number operator,

$$H_{\text{int}} = \frac{\hbar [d^2 - \frac{\hbar}{mv}(b^\dagger b + \frac{1}{2})]}{4d^2 C_{\text{eq}} \sqrt{L_1 L_2 \tilde{\omega}_1 \tilde{\omega}_2}} (a_1^\dagger + a_1)(a_2^\dagger + a_2), \quad (7)$$

and  $H_d$  is the Hamiltonian due to the voltage induced by the NEMS oscillations,

$$H_d = \sqrt{\frac{\hbar}{8}} V_{C_T}(t) \left[ \frac{(a_1^\dagger + a_1)}{\sqrt{L_1 \tilde{\omega}_1}} + \frac{(a_2^\dagger + a_2)}{\sqrt{L_2 \tilde{\omega}_2}} \right]. \quad (8)$$

Assuming the two TLR fields are in resonance,  $\tilde{\omega}_1 = \tilde{\omega}_2 = \tilde{\omega}$ , in a referential rotating with  $\tilde{\omega}$  we can neglect the rapidly oscillating terms appearing in the transformed  $H_d$  and  $H_{\text{int}}$  to obtain (see Appendix C)

$$H_{\text{int}}^I = \hbar(\theta_0 + \theta b^\dagger b)(a_1^\dagger a_2 + a_1 a_2^\dagger), \quad (9)$$

where  $\theta_0 = \frac{\tilde{\omega} \tilde{C}_1}{4C_{\text{eq}}} (1 - \frac{\hbar}{2d^2 mv}) \approx \frac{\tilde{\omega} \tilde{C}_1}{4C_{\text{eq}}}$ , and  $\theta \equiv -\frac{\hbar}{d^2 mv} \theta_0$ . Accordingly with the same assumptions for derivation of Eq. (3),  $\theta \approx 10^{-6} \theta_0$  and therefore is very small, but now we keep it since we show that important features appear due to the effects of the coupling mediated by the NEMS vibration. Hamiltonian (9) shows the effective coupling between the two TLR modes mediated by the NEMS phonon number and allows two direct applications which are discussed in what follows: (i) the QND measurement of the NEMS phonon number and (ii) the generation of a tripartite entanglement involving the mechanical oscillator and the TLR fields, working as a probe of the quantum character of oscillation of the mechanical device.

### III. QND MEASUREMENT OF NEMS PHONON NUMBER

As a first application we develop a scheme for mean phonon number QND measurement [17] of the NEMS through a measurement carried out in one of the TLRs. Let us assume that an external drive  $\mathcal{F}$  (resonant with  $\tilde{\omega}$ ) is applied on TLR 2. The effective interaction Hamiltonian (9) together with this external drive is then given by

$$H_I = \hbar(\mathcal{F}^* a_2 + \mathcal{F} a_2^\dagger) + \hbar(\theta_0 + \theta b^\dagger b)(a_1^\dagger a_2 + a_1 a_2^\dagger). \quad (10)$$

The quantum stochastic differential equations (QSDEs) governing the evolution of  $a_1$  and  $a_2$  are

$$\frac{da_1}{dt} = -i\theta_0 a_2 - i\theta b^\dagger b a_2 - \frac{\kappa_1}{2} a_1 + \sqrt{\kappa_1} a_{1\text{in}}, \quad (11)$$

$$\frac{da_2}{dt} = -i\theta_0 a_1 - i\theta b^\dagger b a_1 - \frac{\kappa_2}{2} a_2 - i\mathcal{F} + \sqrt{\kappa_2} a_{2\text{in}}, \quad (12)$$

where for  $j = 1, 2$ ,  $\kappa_j$  is the relaxation rate, and  $a_{jin}$  is the corresponding noise operator induced by individual reservoirs for the radiation mode at TLR  $j$ . In the limit where  $\theta_0/\kappa_2, \theta/\kappa_2 \ll 1$  the radiation mode in TLR 2 relaxes to a stationary coherent state due to the driving field. However, it affects the radiation mode in TLR 1 as given by Eq. (11) contributing with an additional noise term. In that situation the first two terms in the second member of Eq. (12) can be neglected. The steady state of the radiation mode in TLR 2 is then given by

$$\langle a_2 \rangle \approx \frac{-2i\mathcal{F}}{\kappa_2} \equiv \alpha_2.$$

We assume (without loss of generality) a purely imaginary driving field  $\mathcal{F}$ , so that  $\alpha_2$  is real. We now take into account the residual effect of  $(\theta_0/\kappa_2)$  as an additional dissipative channel for TLR 1. In that situation, the QSDE for  $a_1$ , Eq. (11), then becomes

$$\frac{da_1}{dt} = -i\theta\alpha_2 b^\dagger b - \frac{\kappa_1}{2}a_1 - \frac{\Gamma}{2}a_1 + \sqrt{\kappa_1}a_{1in} + \sqrt{\Gamma}\tilde{a}_{1in}, \quad (13)$$

where  $\Gamma = 2\theta_0^2/\kappa_2$ , and  $\tilde{a}_{1in}$  is an additive quantum noise term. Equation (13) can be exactly solved to give

$$\begin{aligned} a_1(t) = & a_1(0)e^{-\frac{\Gamma+\kappa_1}{2}t} - \frac{2i\alpha_2\theta b^\dagger b}{\Gamma + \kappa_1}(1 - e^{-\frac{\Gamma+\kappa_1}{2}t}) \\ & + \sqrt{\kappa_1} \int_0^t e^{\frac{\kappa_1+\Gamma}{2}(t-t')} a_{1in}(t') dt' \\ & + \sqrt{\Gamma} \int_0^t e^{\frac{\kappa_1+\Gamma}{2}(t-t')} \tilde{a}_{1in}(t') dt'. \end{aligned} \quad (14)$$

What is mostly relevant in this last equation is the contribution of the TLR 2 radiation field amplitude  $\alpha_2$  to the coupling to the mechanical mode. In fact even though  $\theta$  is very small compared to  $\theta_0$  the stationary coherent field  $\alpha_2$  can be made strong enough (through the driving field) to amplify the interaction between the quantum radiation mode in TLR 1 and the mechanical mode. This coupling can indeed be explored to give a measurable experimental quantity. For example, the average photocurrent in TLR 1, defined as  $\langle I_1(t) \rangle = i\sqrt{\hbar\omega}/2L \langle a_1^\dagger - a_1 \rangle$ , can be calculated to give (assuming  $\langle a_1(0) \rangle = 0$ , without loss of generality)

$$\langle I_1(t) \rangle = -\frac{\alpha_2\theta\sqrt{8\hbar\omega}}{\sqrt{L}(\Gamma + \kappa_1)} n_b (1 - e^{-\frac{\Gamma+\kappa_1}{2}t}) \quad (15)$$

with  $n_b = \langle b^\dagger b \rangle$ . To illustrate the TLR 2 photonic current profile in Fig. 3 we plot  $\langle I_1(t) \rangle$  by varying the NEMS average phonon number. It is clearly seen that the average number of phonons in the NEMS produces distinguishable values for the saturation of the photonic current. On the other hand, it is immediate to see that the current variance,  $\langle (\Delta I_1)^2 \rangle = \langle I_1^2 \rangle - \langle I_1 \rangle^2$ , is proportional to the variance of the phonon number,  $\langle (\Delta b^\dagger b)^2 \rangle$ . Therefore, it can be used to infer the number statistics of the mechanical system. This subject is going to be considered further elsewhere.

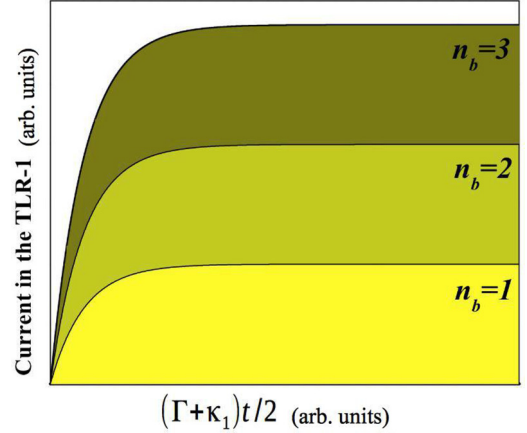


FIG. 3. (Color online) The photonic current  $\langle I_1 \rangle(t)$  in TLR 1, as given by Eq. (15) for three values of the NEMS Fock states with average phonon number  $n_b = 1, 2, 3$ . For  $t \gg 2/(\kappa_1 + \Gamma)$ , all three curves reach a stationary threshold given by the phonon number  $n_b$  in TLR 1 (remembering that  $\theta < 0$ ).

#### IV. ENTANGLEMENT GENERATION

Now we analyze the distribution of entanglement in our tripartite system, as governed by the full quantized Hamiltonian (9). Since  $b^\dagger b$  is a conserved quantity we can solve the Heisenberg equations of motion for the operators  $a_1$  and  $a_2$  to obtain

$$a_k(t) = \sqrt{1 - \mathcal{T}} a_k(0) - i\sqrt{\mathcal{T}} a_j(0), \quad j \neq k, \quad (16)$$

for  $j, k = 1, 2$ . This is exactly the equation for a beam splitter with intensity-dependent transmittance [17]  $\mathcal{T} = \sin^2[(\theta_0 + \theta \langle b^\dagger b \rangle t)]$ . It is well known that a beam splitter entangles only bosonic fields which are nonclassical in the quantum optical sense [18–20], i.e., when at least one of the individual inputs is described by a negative Glauber-Sudarshan  $P$  distribution. For that reason the term in  $\mathcal{T}$  depending on  $\theta_0$  does not entangle the two radiation modes if they are initially in a classical state and therefore can be neglected for simplicity. The transmittance term dependent on the NEMS phonon number, however, allows the three modes, the mechanical and the photonic ones, to be entangled, even when their initial states are classical.

To illustrate this feature, let us consider that the system is prepared in a triple product of coherent states for the NEMS (index  $N$ ) and for the two TLRs (indices 1, 2). Those states are easily generated in the TLRs [by a classical source of radiation such as the one in Eq. (10)] and can in principle be generated in the NEMS with a similar external driving. The joint pure initial state

$$|\psi(0)\rangle = |\alpha\rangle_N |\beta\rangle_1 |\gamma\rangle_2 \quad (17)$$

is a genuine example of a classical tripartite state, but the evolution will generate the conditioned entangled state

$$|\psi(t)\rangle = \sum_{n=0}^{\infty} C_n |n\rangle_N |\beta_n(t)\rangle_1 |\gamma_n(t)\rangle_2, \quad (18)$$

where  $|n\rangle$  are the Fock state, with  $C_n = e^{-\frac{1}{2}|\alpha|^2} \alpha^n / \sqrt{n!}$ , and

$$\begin{aligned}\beta_n(t) &= \beta \cos(n\theta t) - i\gamma \sin(n\theta t), \\ \gamma_n(t) &= \gamma \cos(n\theta t) - i\beta \sin(n\theta t).\end{aligned}\quad (19)$$

For example, considering  $\theta t = \pi$ , the state in Eq. (18) becomes

$$|\psi(t)\rangle = |\alpha_+\rangle_N |\beta\rangle_1 |\gamma\rangle_2 + |\alpha_-\rangle_N |-\beta\rangle_1 |-\gamma\rangle_2, \quad (20)$$

where  $|\alpha_\pm\rangle \propto (|\alpha\rangle \pm |-\alpha\rangle)$  are the even (+) and odd (−) coherent states. So, not only are the three modes entangled, but the NEMS is also left in a mesoscopic Schrödinger cat-like state conditioned on the state on the TLR modes.

In a general way, when tracing over the partition  $N$  in Eq. (18), one can see that the reduced state  $\hat{\rho}_{12}$  is separable; i.e., the NEMS is not able to generate entanglement between the TLRs. However, an easy inspection of Eq. (18) or even Eq. (20) shows that when tracing over 1 or 2 the remaining system is entangled due to the nonorthogonality of coherent states, being nonentangled only for large  $\beta$  and  $\gamma$ . Following the classification of [21] this is a *one-part separable state*. For pure global states, the universal measure of entanglement is the von Neumann entropy, or the purity as given by the linear entropy  $E_{A|B} = 1 - \text{Tr} \hat{\rho}_B^2$ . Here  $\hat{\rho}_B$  represents the reduced density operator after tracing over the part  $A$  of the total system with  $\hat{\rho} = |\psi(t)\rangle\langle\psi(t)|$ . The behavior of the bipartitions from Eq. (18) are encoded in the following equations for linear entropies:

$$E_{N|12} = 1 - \sum_{n,m=0}^{\infty} |C_n|^2 |C_m|^2 e^{-|\beta_n - \beta_m|^2 - |\gamma_n - \gamma_m|^2}, \quad (21)$$

$$E_{1|N2} = 1 - \sum_{n,m=0}^{\infty} |C_n|^2 |C_m|^2 e^{-|\beta_n - \beta_m|^2}, \quad (22)$$

$$E_{2|N1} = 1 - \sum_{n,m=0}^{\infty} |C_n|^2 |C_m|^2 e^{-|\gamma_n - \gamma_m|^2}. \quad (23)$$

By the Poissonian nature of  $|C_n|^2$  and the boundedness of the exponentials, all above sums are convergent. In Figs. 4 and 5 we show  $E_{N|12}$  for some initial coherent states when the summation is realized over 30 terms—the error in this truncation is of the order of  $10^{-17}$  for all the plotted curves. As one can see, although the system recurs to a nonentangled state after a period, it is usually highly entangled. At  $\theta t = l\pi$ , with  $l = 1, 3, 5, \dots$ , the state is as in Eq. (20). This is a simple scheme for tripartite entanglement generation involving mechanical and photonic modes in a continuous-variables regime, which can be easily implemented in a circuit.

This situation for the global pure state is useful for extension to the case when the NEMS is in an arbitrary state

$$\rho_N = \int d^2\alpha P(\alpha) |\alpha\rangle\langle\alpha|, \quad (24)$$

in terms of the Glauber-Sudarshan  $P$  distribution  $P(\alpha)$ , and the two TLRs are again prepared in coherent states  $|\beta\rangle_1$  and  $|\gamma\rangle_2$ . For that case the joint evolved state is given by

$$\begin{aligned}\rho &= \int d^2\alpha \sum_{n,m=0}^{\infty} P(\alpha) C_n C_m^* \\ &\quad \times |n, \beta_n(t), \gamma_n(t)\rangle\langle m, \beta_m(t), \gamma_m(t)|_{N12}.\end{aligned}\quad (25)$$

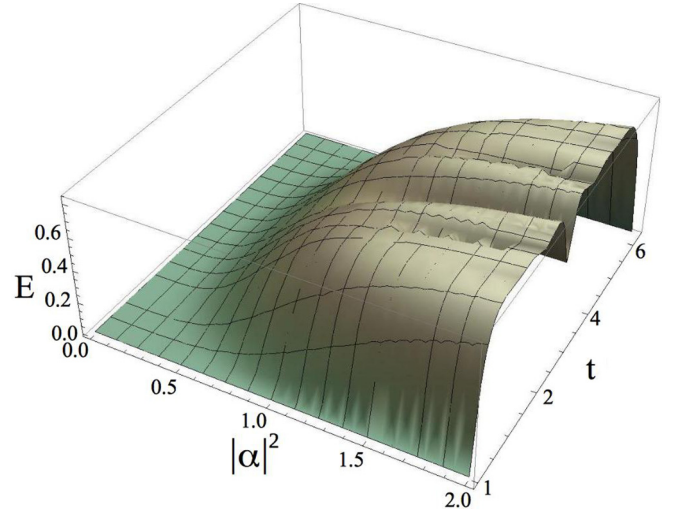


FIG. 4. (Color online) Linear entropy of the partition  $N|12$  quantifying the entanglement between the NEMS and the two TLRs as a function of time  $t$  (here normalized with  $\Gamma$ ) and  $|\alpha|$ . We choose  $\alpha = \beta = \gamma \in \mathbb{R}$ . Note the entanglement's recurrence due to the  $2\pi$ -periodic behavior of the functions in Eqs. (19).

However, the previous analysis in terms of the marginal entropies cannot be applied here since the global state can be mixed, and one has to resort to continuous-variable methods for entanglement detection [22–24]. It is not difficult to infer that the tripartite state will be entangled for a broad range of NEMS states. For example, when it is in a thermal state,  $P(\alpha) = (\pi\bar{n})^{-1} e^{-|\alpha|^2/\bar{n}}$  is a regular Gaussian function, where  $\bar{n}$  is the average number of thermal phonons. Therefore, the NEMS state is classical, but after the evolution the tripartite state is non-Gaussian and can be entangled or not depending on  $\bar{n}$ . We remark that since the global state is non-Gaussian, the entanglement detection requires a more detailed analysis dealing with the actual experimental limitations at hand. This is left for further investigation.

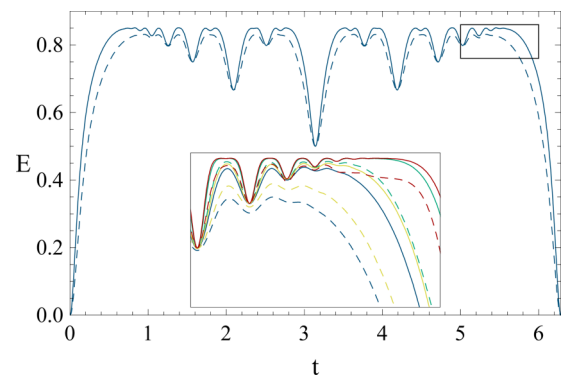


FIG. 5. (Color online) Linear entropy of the partitions  $N|12$  (solid) and  $1|N2$  (dashed) for  $\alpha = \beta = \gamma = 2$  as a function of time  $t$  (here normalized with  $\Gamma$ ). Since  $\beta = \gamma$ ,  $E_{1|N2} = E_{2|N1}$ . Inset: The same linear entropies for distinct values of the initial state for  $\alpha = 2$  and  $\beta = \gamma = 2$  (blue);  $\beta = 3, \gamma = 4$  (green);  $\beta = \gamma = 1 + 2i$  (yellow); and  $\beta = 3 + 4i, \gamma = 1 + 2i$  (red).

## V. SUMMARY

In conclusion, in this paper we have investigated the possibility to directly couple capacitively two TLRs and a NEMS. The important feature here is that by treating the three parts of the system quantum mechanically we could obtain an interaction Hamiltonian that couples the NEMS phonon number to the charges of the TLRs. We have considered two simple applications of this setup. First, the circuit may be considered for QND detection of the average number of phonons in the NEMS by photonic currents at one of the TLRs. We have shown that depending on NEMS average phonon number the current at one of the TLRs will furnish a characteristic and distinguishable behavior. This is quite important for actual detection schemes, since it is independent in principle of the inherent frequencies in the system. A second application is devised as a beam splitter conditioned to the NEMS phonon number and this is employed in a scheme for generation of tripartite entanglement for a continuous-variables system. This kind of device, an intensity-conditioned beam splitter, is nonexistent for optical fields and could in principle be used for quantum-information processing or detection purposes.

## ACKNOWLEDGMENTS

This work is supported in part by CAPES and by FAPESP, and CNPq through the National Institute for Science and Technology of Quantum Information and through the Research Center in Optics and Photonics (CePOF). G.J.M. acknowledges the support of the [Australian Research Council](#) Grant No. [CE110001013](#). M.C.O. acknowledges insightful comments and suggestions made by M. LaHaye. O.P.S.N. is grateful to L. D. Machado, S. S. Coutinho, and K. M. S. Garcez for helpful discussions.

## APPENDIX A: DERIVATION OF HAMILTONIAN (1)

Considering the source voltage for the circuit in Fig. 2,  $V_{L_1} + V_{C_1} + V_{C_L} = V_{L_2} + V_{C_2} + V_{C_R}$ , we arrive at the equations for the charge:

$$L_1 \frac{d^2}{dt^2} Q_1(t) + \frac{1}{C_1} Q_1(t) = -\frac{Q_L(t)}{C_L(t)}, \quad (\text{A1})$$

$$L_2 \frac{d^2}{dt^2} Q_2(t) + \frac{1}{C_2} Q_2(t) = -\frac{Q_R(t)}{C_R(t)}. \quad (\text{A2})$$

Considering the total current in the system,  $I(t) = I_1 + I_2$ , we obtain

$$I(t) = \frac{d}{dt} Q_1(t) + \frac{d}{dt} Q_2(t) = \frac{d}{dt} Q_L(t) + \frac{d}{dt} Q_R(t), \quad (\text{A3})$$

or

$$Q_1(t) + Q_2(t) = Q_L(t) + Q_R(t) + K, \quad (\text{A4})$$

where  $K$  is a constant which we assume as null, without any loss of generality. Moreover, the voltage over the whole capacitor is given by

$$V_{C_T} = V_{C_L} - V_{C_R} = \frac{Q_L(t)}{C_L(t)} - \frac{Q_R(t)}{C_R(t)}. \quad (\text{A5})$$

Combining Eqs. (A4) and (A5), we obtain

$$Q_L(t) = \frac{C_T}{C_R(t)} (Q_1(t) + Q_2(t)) + C_T V_{C_T}(t), \quad (\text{A6})$$

$$Q_R(t) = \frac{C_T}{C_L(t)} (Q_1(t) + Q_2(t)) - C_T V_{C_T}(t), \quad (\text{A7})$$

where  $C_T^{-1} = C_L^{-1}(t) + C_R^{-1}(t) = \frac{2d}{\epsilon_0 A} = 2C_{\text{eq}}^{-1}$ .

Inserting Eqs. (A6) and (A7) in Eqs. (A1) and (A2), we obtain

$$L_1 \frac{d^2}{dt^2} Q_1(t) + \left( \frac{1}{C_1} + \frac{C_T}{C_L(t)C_R(t)} \right) Q_1(t) + \frac{C_T}{C_L(t)C_R(t)} Q_2(t) = -\frac{C_T}{C_L(t)} V_{C_T}(t), \quad (\text{A8})$$

$$L_2 \frac{d^2}{dt^2} Q_2(t) + \left( \frac{1}{C_2} + \frac{C_T}{C_L(t)C_R(t)} \right) Q_2(t) + \frac{C_T}{C_L(t)C_R(t)} Q_1(t) = +\frac{C_T}{C_R(t)} V_{C_T}(t). \quad (\text{A9})$$

Now, using the definitions for  $C_L(t)$ ,  $C_R(t)$  (see the main text) and  $C_T$  given below Eq. (A7), we have

$$\frac{C_T}{C_L(t)C_R(t)} = \frac{(d^2 - x^2(t))}{2d\epsilon_0 A}, \quad (\text{A10})$$

and

$$\frac{C_T}{C_L(t)} = \frac{(d - x(t))}{2d}, \quad \frac{C_T}{C_R(t)} = \frac{(d + x(t))}{2d}. \quad (\text{A11})$$

By defining

$$\frac{1}{\tilde{C}_i} \equiv \frac{1}{C_i} + \frac{(d^2 - x^2(t))}{2d\epsilon_0 A}, \quad (\text{A12})$$

the canonical variables in the circuit  $P_i(t) = L_i \dot{Q}_i = L_i I_i(t)$ . Equations (A8) and (A9) can be written as

$$\frac{d}{dt} Q_1(t) = \frac{1}{L_1} P_1(t), \quad (\text{A13})$$

$$\frac{d}{dt} P_1(t) = -\frac{1}{\tilde{C}_1} Q_1(t) - \frac{[d^2 - x^2(t)]}{2d\epsilon_0 A} Q_2(t) - \frac{[d - x(t)]}{2d} V_{C_T}(t), \quad (\text{A14})$$

$$\frac{d}{dt} Q_2(t) = \frac{1}{L_2} P_2(t), \quad (\text{A15})$$

$$\frac{d}{dt} P_2(t) = -\frac{1}{\tilde{C}_2} Q_2(t) - \frac{[d^2 - x^2(t)]}{2d\epsilon_0 A} Q_1(t) + \frac{[d + x(t)]}{2d} V_{C_T}(t), \quad (\text{A16})$$

which, finally, allow us to derive the system Hamiltonian (1).

## APPENDIX B: DERIVATION OF HAMILTONIAN (5)

Two situations must be analyzed, when the NEMS behaves quantum mechanically and when it behaves classically. Since the classical description can be derived from the

quantum one we only describe the last one and later recast the classical behavior. By writing  $x(t) = \sqrt{\frac{\hbar}{2mv}}(be^{-i\omega t} + b^\dagger e^{i\omega t})$  we obtain  $x^2(t) = \frac{\hbar}{2mv}[b^2 e^{-i2\omega t} + (b^\dagger)^2 e^{i2\omega t} + 2b^\dagger b + 1]$ . For rapid oscillations ( $\omega t \gg 1$ ),  $x(t) \approx 0$ , and  $x^2(t) \approx \frac{\hbar}{mv}(b^\dagger b + \frac{1}{2}) \equiv x_{\text{rms}}^2$ . Thus,

$$\frac{1}{\tilde{C}_i} = \frac{1}{C_i} + \frac{d^2 - \frac{\hbar}{mv}((b^\dagger b) + \frac{1}{2})}{2d\epsilon_0 A}. \quad (\text{B1})$$

Dividing both sides of Eq. (B1) by  $L_i$  we obtain a relation between the two frequencies  $\omega_i^2 \equiv (L_i C_i)^{-1}$  and  $\tilde{\omega}_i^2 \equiv (L_i \tilde{C}_i)^{-1}$  as

$$\tilde{\omega}_i^2 = \omega_i^2 + \frac{d^2 - x_{\text{rms}}^2}{2d\epsilon_0 A L_i}, \quad (\text{B2})$$

or

$$\tilde{\omega}_i^2 = \omega_i^2 + \frac{\omega_{i,\text{eq}}^2}{2} \left(1 - \frac{x_{\text{rms}}^2}{d^2}\right), \quad (\text{B3})$$

with  $\omega_{i,\text{eq}}^2 \equiv (C_{\text{eq}} L_i)^{-1}$ . We assume  $d \approx 10^{-8}$  m,  $x_{\text{rms}}^2/d^2 = 10^{-6}$  [15,16], and so it can be disregarded from Eq. (3). Typical experimental values settle  $\omega_i = 6$  GHz, and whenever the second term in Eq. (3) is of the same order it should be taken into account. In any case in  $\tilde{\omega}_i^2$  we keep the maximal value the second term can take; i.e., we adopt  $\tilde{\omega}_i^2 = \omega_i^2 + \omega_{i,\text{eq}}^2/2$ , meaning that

$$\frac{1}{\tilde{C}_i} = \frac{1}{C_i} + \frac{1}{2C_{\text{eq}}}. \quad (\text{B4})$$

Thus, Hamiltonian (1) reduces to

$$\begin{aligned} \mathcal{H} \approx & \frac{P_1^2}{2L_1} + \frac{Q_1^2}{2\tilde{C}_1} + \frac{P_2^2}{2L_2} + \frac{Q_2^2}{2\tilde{C}_2} \\ & + \frac{d^2 - \frac{\hbar}{mv}(b^\dagger b + 1/2)}{2d\epsilon_0 A} Q_1 Q_2 \\ & + \frac{1}{2} V_{C_T}(t) Q_1 - \frac{1}{2} V_{C_T}(t) Q_2. \end{aligned} \quad (\text{B5})$$

Finally by assuming the conjugate variables (4), which follow the standard commutation relation, we thus obtain Hamiltonian (5).

### APPENDIX C: DERIVATION OF HAMILTONIAN (9)

Let us assume in Hamiltonian (5) that the two TLRs are at resonance with frequency  $\tilde{\omega}_1 = \tilde{\omega}_2 = \tilde{\omega}$ , meaning here that  $C_1 = C_2$  and  $L_1 = L_2$ . Now we transform to a referential rotating with  $\tilde{\omega} : U H U^\dagger$ ,  $U = \exp[-i\tilde{\omega}t(a_1^\dagger a_1 + a_2^\dagger a_2)]$ , such that

$$\begin{aligned} H_{\text{int}}^I &= \hbar(\theta_0 - \theta b^\dagger b) \\ &\times (a_1 a_2 e^{-2i\tilde{\omega}t} + a_1^\dagger a_2^\dagger e^{2i\tilde{\omega}t} + a_1^\dagger a_2 + a_1 a_2^\dagger), \end{aligned} \quad (\text{C1})$$

and

$$\begin{aligned} H_d^I &= \sqrt{\frac{\hbar}{8\tilde{\omega}L_1}} V_{C_T}(t) \\ &\times [(a_1^\dagger + a_2^\dagger)e^{i\tilde{\omega}t} + (a_1 + a_2)e^{-i\tilde{\omega}t}] \end{aligned} \quad (\text{C2})$$

with  $\theta_0 = \frac{\tilde{\omega}\tilde{C}_1}{4C_{\text{eq}}}(1 - \frac{\hbar}{2d^2mv}) \approx \frac{\tilde{\omega}\tilde{C}_1}{4C_{\text{eq}}}$ , and  $\theta \equiv -\frac{\hbar}{d^2mv}\theta_0$ . For frequencies  $\tilde{\omega}$  at the gigahertz scale the oscillating terms in Eqs. (C1) and (C2) can be dropped and the remaining time-independent term is exactly Hamiltonian (9).

- 
- [1] N. Bohr, Usp. Fiz. Nauk **66**, 571 (1958).  
[2] R. G. Knobel and A. N. Cleland, *Nature (London)* **424**, 291 (2003).  
[3] M. D. LaHaye, O. Buu, B. Camarota, and K. C. Schwab, *Science* **304**, 74 (2004).  
[4] A. Naik, O. Buu, M. D. LaHaye, A. D. Armour, A. A. Clerk, M. P. Blencowe, and K. C. Schwab, *Nature (London)* **443**, 193 (2006).  
[5] M. D. LaHaye, J. Suh, P. M. Echternach, K. C. Schwab, and M. L. Roukes, *Nature (London)* **459**, 960 (2009).  
[6] J. D. Teufel, T. Donner, M. A. Castellanos-Beltran, J. W. Harlow, and K. W. Lehnert, *Nat. Nanotechnol.* **4**, 820 (2009).  
[7] A. D. O'Connell, M. Hofheinz, M. Ansmann, R. C. Bialczak, M. Lenander, E. Lucero, M. Neeley, D. Sank, H. Wang, M. Weides *et al.*, *Nature (London)* **464**, 697 (2010).  
[8] J. Chan, T. P. M. Alegre, A. H. Safavi-Naeini, J. T. Hill, A. Krause, S. Gröblacher, M. Aspelmeyer, and O. Painter, *Nature (London)* **478**, 89 (2011).  
[9] D. V. Seletskiy, M. P. Hehlen, R. I. Epstein, and M. Sheik-Bahae, *Adv. Opt. Photon.* **4**, 78 (2012).  
[10] J. Hertzberg, T. Rocheleau, T. Ndukum, M. Savva, A. Clerk, and K. Schwab, *Nat. Phys.* **6**, 213 (2010).  
[11] L. F. Wei, Y.-x. Liu, C. P. Sun, and F. Nori, *Phys. Rev. Lett.* **97**, 237201 (2006).  
[12] X. Zhou and A. Mizel, *Phys. Rev. Lett.* **97**, 267201 (2006).  
[13] G. J. Milburn, C. A. Holmes, L. M. Kettle, and H. S. Goan, in *Proceedings of the QCMC06*, edited by O. Hirota and J. Shapiro (Rinton Press, Paramus, NJ, 2007).  
[14] J. Teufel, T. Donner, D. Li, J. Harlow, M. Allman, K. Cicak, A. Sirois, J. Whittaker, K. Lehnert, and R. Simmonds, *Nature (London)* **475**, 359 (2011).  
[15] L. Frunzio, A. Wallraff, D. Schuster, J. Majer, and R. Schoelkopf, *IEEE Trans. Appl. Supercond.* **15**, 860 (2005).  
[16] K. C. Schwab and M. L. Roukes, *Phys. Today* **58**, 36 (2005).  
[17] D. F. Walls and G. G. J. Milburn, *Quantum Optics* (Springer, New York, 2007).  
[18] M. S. Kim, W. Son, V. Bužek, and P. L. Knight, *Phys. Rev. A* **65**, 032323 (2002).  
[19] Xiang-bin Wang, *Phys. Rev. A* **66**, 024303 (2002).  
[20] M. de Oliveira and W. Munro, *Phys. Lett. A* **320**, 352 (2004).  
[21] W. Dür, J. I. Cirac, and R. Tarrach, *Phys. Rev. Lett.* **83**, 3562 (1999).  
[22] M. C. de Oliveira, *Phys. Rev. A* **72**, 012317 (2005).  
[23] M. C. de Oliveira, F. Nicacio, and S. S. Mizrahi, *Phys. Rev. A* **88**, 052324 (2013).  
[24] F. Nicacio and M. C. de Oliveira, *Phys. Rev. A* **89**, 012336 (2014).